Ordering Dynamics of a Symmetric Polystyrene-*block*-polyisoprene. 1. Ordering Mechanism from the Disordered State

Naoki Sakamoto and Takeji Hashimoto*

Department of Polymer Chemistry, Graduate School of Engineering, Kyoto University, Kyoto 606-8501, Japan

Received November 24, 1997; Revised Manuscript Received March 10, 1998

ABSTRACT: We have investigated the ordering dynamics and mechanism of a nearly symmetric polystyrene-*block*-polyisoprene by quenching the specimen from a temperature above the order−disorder transition temperature, T_{ODT}, to temperatures below T_{ODT}, by using time-resolved small-angle X-ray scattering (SAXS) and transmission electron microscopy (TEM) as a function of quench depths. The time-resolved SAXS revealed that the ordering at shallow quenches proceeds via nucleation and growth process as follows: (I) after quenching the specimen, the thermal concentration fluctuations relax rapidly from the initial state to the disordered state at the temperature very close to T_{ODT} within the shortest time covered in this experiment; (II) the system stays in this disordered state for a certain incubation period; (III) after this period, the lamellar microdomains are nucleated and grow. This ordering mechanism is essentially same at any quench depths covered in this experiments, except for the largest quench depth. Furthermore the Avrami analysis together with TEM observations revealed that the nucleation occurs *homogeneously* and generates a highly *anisotropic* shape of grains composed of lamellae with their size parallel to lamellar normals being much greater than that normal to them.

I. Introduction

The order−disorder transition (ODT) of block copolymer melts has been extensively studied[1] since Leibler's pioneering theory[2] was proposed. The theory predicts that the scattered intensity $I(q)$ at scattering vector $\mathbf{q}$ in the disordered state is given by

$$[I(q)/N]^{-1} \sim F(q) - 2\chi N \tag{1}$$

where N and χ are the total degree of the polymerization of block copolymers and the Flory−Huggins segmental interaction parameter, respectively. The quantity q is defined by

$$q = (4\pi/\lambda)\sin(\theta/2) \tag{2}$$

where λ and θ are the wavelength of incident radiation and scattering angle in the medium, respectively. The function $F(q)$ depends on radius of gyration R_g and composition, f, of a block copolymer. Recently some important theoretical[3,4] and experimental[5−9] results were obtained for block copolymer melts having relatively weak segregation power, χN. These results conclude that the random thermal force neglected in Leibler's mean-field theory plays a very important role on ODT and the scattering behaviors near the ODT temperature, T_{ODT}.

Figure 1 schematically shows the reciprocal of the maximum intensity, I_m^{-1}, the square of half-width at half-maximum of the first-order peak, σ_q^2, and the characteristic length, D, obtained from small-angle X-ray scattering (SAXS) or small-angle neutron scattering (SANS) profiles, plotted as a function of the reciprocal of the absolute temperature, $1/T$. The length D is given by $D = 2\pi/q_m$, where q_m is magnitude of the scattering vector at the first-order scattering maximum. Leibler's mean-field theory predicted that I_m^{-1} and σ_q^2 decrease linearly with $1/T$ if χ changes linearly with $1/T$, and the temperature dependence of D is equal to that of an unperturbed chain dimension, $R_{g0}(T)$, of a block copolymer in the disordered state. In Figure 1, $D_r(T)$ is defined by $D_r(T) \equiv D(T_r)[R_{g0}(T)/R_{g0}(T_r)]$ where T_r is a given reference temperature in the disordered state. $D_r(T)$ shows the temperature dependence of D predicted by the mean-field theory.

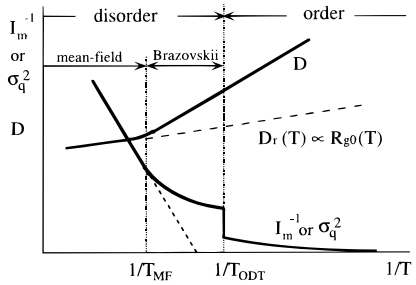

Figure 1. Schematic representation of I_m^{-1}, σ_q^2, and D, obtained by SAXS or SANS, plotted as a function of $1/T$ in block copolymer systems with relatively low molecular weight.

At sufficiently high temperature, I_m^{-1}, σ_q^2, and D have been found to vary as predicted by the mean-field theory.[8] However with increasing $1/T$ close to $1/T_{ODT}$, I_m^{-1} and σ_q^2 start to deviate from the linear relationship, showing a downward convex curvature, and the temperature dependence of D becomes larger than $D_r(T)$. These deviations from the mean-field behavior have been elucidated to be due to the thermal force effect (the Brazovskii effect[10]), and the upward deviation of I_m^{-1} and σ_q^2 indicates that the random thermal force suppresses the concentration fluctuations of the component polymer segments. We referred to the crossover temperature from the mean-field to the non-mean-field behavior as T_{MF} for the sake of convenience.[8] The values of I_m^{-1} and σ_q^2 change discontinuously at T_{ODT}. Until recent years D had been considered to show essentially no change at T_{ODT} in a symmetric or nearly symmetric diblock copolymer system forming lamellar microdomains in the ordered state,[6−8] though it was found to change discontinuously in an asymmetric block copolymer system.[9,11] However very recently it was

S0024-9297(97)01720-8 CCC: $15.00
Published on Web 04/24/1998

Table 1. Molecular Characteristics of the Polystyrene-*block*-polyisoprene Diblock Copolymers

code	$10^{-4}M_n$	M_w/M_n	f_{PS}[a]	T_{ODT} (°C)
OSI-3	1.5	1.02	0.45	98.5[b]−100.1[c]
SS-7	1.9	1.02	0.46	141[b]−145[c]

[a] f_{PS} is volume fraction of polystyrene block chains. [b] Onset temperature of disordering. [c] Completion temperature of disordering.

found that D shows a discontinuity even in the nearly symmetric block copolymer, though the discontinuity is very small.[12] The discontinuous change in I_m^{-1} and σ_q^2 at T_{ODT} manifests that the ODT is the first-order phase transition and that the random thermal force plays an important role on the phase transition.

Fredrickson and Binder[13] proposed the theory of the ordering dynamics of the ODT. In the context of Leibler's mean field theory,[2] the ODT for a symmetric diblock copolymer belongs to the second-order phase transition in which the transition takes place by *spinodal decomposition*. However Fredrickson and Binder theory predicted that the ordering near ODT can proceed via *nucleation and growth* process even for a symmetric diblock copolymer system, when the thermal noise effect comes into play (thermal-force-induced first-order phase transition[3,10]). Leibler's mean-field theory predicts that the ODT is the second-order phase transition only for the *exactly* symmetric block copolymers. Hence, strictly speaking, the ODT of the *nearly* symmetric block copolymers, which is not exactly symmetric such as the ones employed in the present study (see Table 1), is expected to be the first-order phase transition even in the context of the mean-field theory. Nevertheless the random thermal force strongly affects the ODT and the ordering mechanism near ODT even for the nearly symmetric block copolymers: the effects of the thermal force for the nearly symmetric block copolymers are as important as those for the exactly symmetric block copolymers. The ODT and the ordering process of the nearly symmetric block copolymers may have a theoretical basis essentially identical to that for the exactly symmetric block copolymer.

Since the Fredrickson and Binder theory was proposed, the dynamics of ODT has been attracted considerable attention and has been experimentally studied by means of SAXS,[11,14−17] SANS,[18] low-frequency rheology,[19−21] and depolarized light scattering.[22,23] These experimental results suggested that the ordering of the block copolymer at temperatures close to T_{ODT} proceeds via nucleation and growth process with an incubation period.

However the results obtained previously were not supported by a real-space analysis: there is no attempt to observe the ordering process of a block copolymer by microscopic method such as transmission electron microscopy (TEM). Furthermore the state (or structure) of the system in the incubation period and that during the formation of the ordered microdomains are hardly elucidated. In the previous studies, the time evolution of the volume fraction of the ordered phase used for Avrami analysis was obtained by assuming that the system during the ordering is composed of the disordered phase in the incubation period and the ordered phase at $t \rightarrow \infty$ (i.e., at a long time limit) after quenching the specimen from the disordered state to the ordered state, but this assumption has not been confirmed at all. Moreover in all the previous temperature-drop (T-drop) experiments for examining the ordering mechanism, the specimens were quenched from the temperature just above T_{ODT}; hence, the effects of the initial temperature on the ordering mechanism are not clarified.

In this series of the study, we performed T-drop experiments from the temperature T_i above the T_{MF} ($\gg T_{ODT}$) where the system is in the mean-field disordered state (see Figure 1) for a nearly symmetric polystyrene-*block*-polyisoprene (SI) diblock copolymer having a relatively small N. The ordering process after T-drop was observed by using the combination of time-resolved SAXS and TEM to make reciprocal- and real-space analyses on the ordering process. To clarify the quench-depth dependence of the ordering mechanism, the specimens were quenched to various temperatures, T_fs ($< T_{ODT}$).

In this paper we focus mainly on the following three items: (1) the precise analysis about the states of the system during the ordering process, with SAXS and TEM; (2) the ordering mechanism at different quench depths; (3) Avrami analysis, in which the volume fraction of the ordered phase is obtained by SAXS analysis in item 1.

II. Experimental Methods

SI diblock copolymers coded as OSI-3 and SS-7 were prepared by living anionic polymerization with *sec*-butyllithium as initiator and cyclohexane as a solvent according to the standard method. These polymers have a nearly symmetric composition and form a lamellar structure in the ordered state. Their molecular characteristics were listed in Table 1. Here it should be mentioned that the copolymers employed in the present experiments are not exactly symmetric (f_{PS} = 0.45 or 0.46). We believe that the block copolymers with f_{PS} of 0.45 or 0.46 has been experimentally regarded as symmetric block copolymers.

The T_g of the polystyrene- (PS-) rich phase in the OSI-3 was measured by DSC. The sample was first brought into a disordered state by annealing at 120 °C for 20 min and cooled from 120 to 0 °C with a cooling rate of 20 °C/min. After keeping the specimen at 0 °C for 20 min, the DSC measurement was done from 0 to 120 °C with a heating rate of 20 °C/min. The cooling and heating process may induce ordering of the specimens to some degree. The T_g thus measured is 61 °C.[24]

To determine the T_{ODT} of OSI-3 and SS-7, we first performed the static SAXS measurements at each temperature with the SAXS apparatus,[25−27] which consists of an 18-kW rotating-anode X-ray generator (MAC Science Co. Ltd., Yokohama, Japan), a graphite crystal for incident-beam monochromatization, a 1.5 m camera (0.5 m from the source to the sample and 1.0 m from the sample to the detector), and a one-dimensional position-sensitive proportional counter (PSPC). The sample temperature was controlled with accuracy of ±0.003 °C with a temperature enclosure and controller constructed in our laboratory. The SAXS was measured during cooling and heating the specimens between 200 and 30 °C. To examine the sharpness of the ODT, the high temperature-resolution measurements (the measurements with a small temperature increment [0.2−1.0 °C]) were performed at the temperatures very close to the T_{ODT}. At each measuring temperature, the specimens were hold for about 30 min before measurements, and SAXS profiles were measured for 30 min. The sample was put in an evacuated chamber to reduce thermal degradation as much as possible.

The T-drop measurements for OSI-3 were conducted by quenching the block copolymer melt from T_i = 172 °C which is above T_{MF} in the mean-field disordered state to T_f which is below T_{ODT} in the ordered state. The T-drop experiment is schematically illustrated in Figure 2a. Figure 2b shows the sample holder made of aluminum. The quenching process was

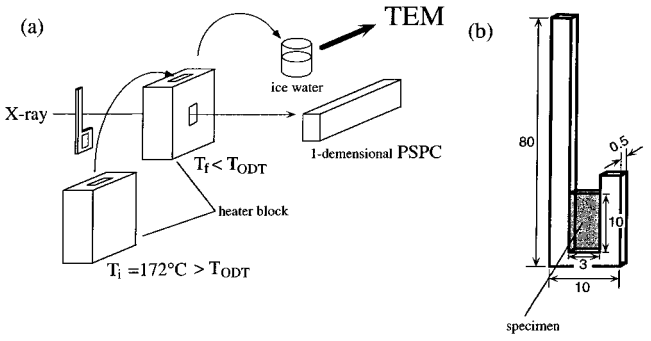

Figure 2. (a) Schematic illustration for the *T*-drop experiment and (b) the sample holder used in this work. The numbers in (b) indicate the size of the sample holder in unit of mm.

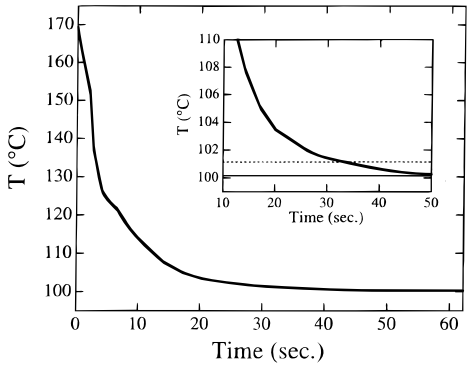

Figure 3. Time change in the temperature at the center of the specimen after *T*-drop from 172 to 100.1 °C. The inset highlights the temperature change near 100.1 °C.

done as follows: (1) the specimen was placed in the sample holder shown in Figure 2b, where the both sides of the window are sealed by Kapton films of 14 μm thickness; (2) the sample holder with the specimen was put in the heater block in which the temperature was controlled at T_i above T_{ODT}; (3) the holder was rapidly transferred manually into the another heater block which was set on the optical path of incident X-ray beam and regulated at T_f; (4) the time-resolved SAXS measurements were started and time t was set to zero at the time when the specimen was put into the heater block at T_f. The SAXS profiles were detected by a one-dimensional PSPC. The profiles obtained were corrected for slit-width and slit-height smearing, absorption, air scattering, and thermal diffuse scattering as described elsewhere.[25−27] The absolute SAXS intensity was obtained using the nickel-foil method.[28] The *T*-drop measurements for SS-7 were conducted with the same manner as that for OSI-3, from T_i = 187 °C which is above T_{ODT} to T_f = 140 and 121 °C which is below T_{ODT}.

To check how long does it take for the specimen to reach the set temperature, T_f, we made the preliminary experiment in which we embedded the thermocouple in the center of the specimen and made the *T*-drop from the T_i of 172 °C to the T_f of 100.1 °C with the same method as described above. The time change in the temperature is given in Figure 3. The temperature of the specimen reaches T_f + 1 °C within 33 s and reaches T_f within 50 s. Thus it is confirmed that the temperature of the specimen will reach the equilibrium after *T*-drop within ca. 50 s.

To conduct a real-space analysis on the ordering process, we made the TEM observations on the time evolution of the structures during the ordering for OSI-3. After *T*-drop from T_i to T_f, the specimen was rapidly quenched into the ice−water bath (0 °C) at particular times during the ordering process (Figure 2). Because the T_g of PS phase in the block copolymer is higher than 0 °C, we could freeze the structure at the moment when the specimen was put into the ice−water bath. Thus we could observe the structures frozen at specified times during the ordering process with TEM. The frozen specimens

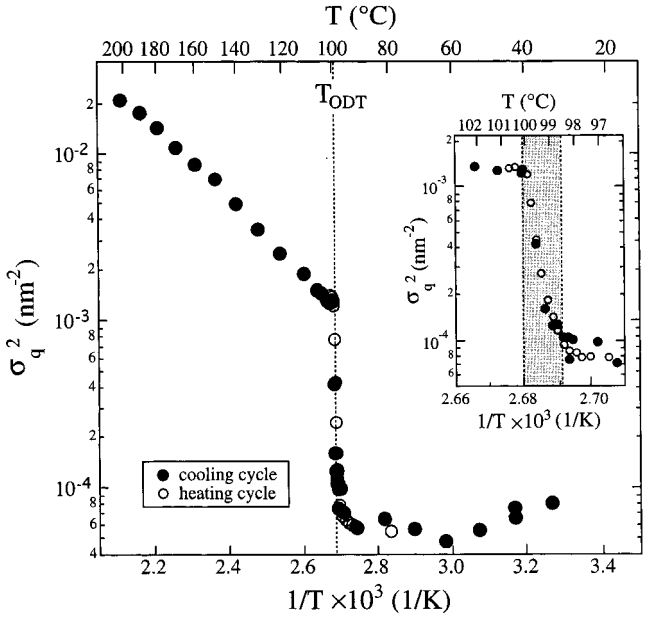

Figure 4. σ_q^2 plotted as a function of 1/*T* for OSI-3. The inset highlights the change in σ_q^2 near T_{ODT}.

were subjected to microtoming into the ultrathin sections of ca. 50 nm thickness at −85 °C with a Reichert-Jung Ultracut E together with a cryogenic unit FC 4E and a glass knife. The ultrathin sections were quickly picked up on 400-mesh copper grids and stained by osmium tetraoxide vapor at room temperature for about a half day. TEM observation was made with a Hitachi H-600 transmission microscope at 100 kV. We confirmed that the SAXS profiles were unchanged before and after freezing process as well as before and after staining, thus ensuring no structural changes during the sample preparation processes for the TEM observations.[29]

III. Experimental Results

III-1. Determination of T_{ODT} and Two-Phase Coexistence Very near T_{ODT}. Figure 4 shows the square of half-width at half-maximum of the first-order peak, σ_q^2, obtained from the SAXS profiles of OSI-3 taken in-situ at various temperatures. A sharp and remarkable change in σ_q^2 is clearly discerned at the temperatures between 98.5 and 100.1 °C. This discontinuous change enables a clear-cut determination of the T_{ODT} in this block copolymer. The T_{ODT} thus determined is 98.5 < T_{ODT} < 100.1 °C. It should be mentioned in this figure that the values σ_q^2 at the temperatures between 98.5 and 100.1 °C are between the value of σ_q^2 at 98.5 and the one at 100.1 °C. Furthermore the SAXS profiles between 98.5 and 100.1 °C can be approximately expressed in terms of a weighted average of the profiles at 100.1 °C, which is the lowest temperature in the disordered state, and at 98.5 °C, which is the highest temperature in the ordered state; i.e., the scattered intensity $I(q)$ at the temperatures between 98.5 and 100.1 °C is described by

$$I(q) = (1 - X_{order})I(q;\ T = 100.1\ °C) + X_{order}I(q;\ T = 98.5\ °C) \quad (3)$$

where $I(q;\ T = T_r)$ is the scattered intensity at a given temperature, T_r.

Figure 5 gives the observed SAXS profile at 99.2 °C (filled circles) and the corresponding calculated profile by eq 3 with X_{order} = 0.62 (solid line). The calculated profile shows a good agreement with the profile mea-

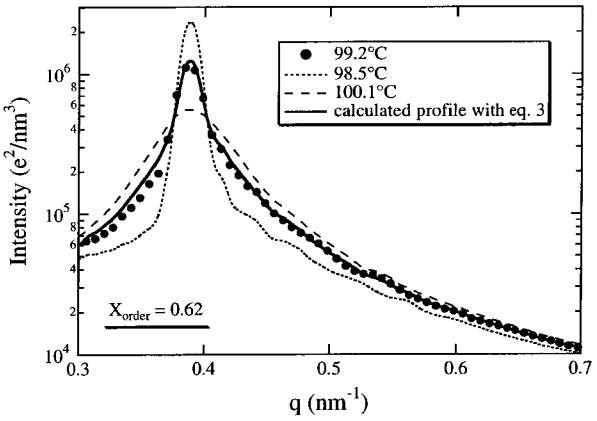

Figure 5. Equilibrium SAXS profile at 99.2 °C for OSI-3 (filled circles). The profile drawn by the solid line shows the profile calculated by eq 3 with $X_{order} = 0.62$. The profiles drawn by the broken and dotted lines show the SAXS profiles of OSI-3 measured at 100.1 and 98.5 °C which are the lower bound for the disordered state and the upper bound for the ordered state, respectively.

sured at 99.2 °C. Thus we conclude that the ordered and disordered phases coexist between 98.5 and 100.1 °C within the time scale of this experiment (ca. 6 h): the two-phase coexistence persists over the temperature interval of 1.6 °C. The X_{order} is related to the volume fraction of the ordered phase in the system. The more precise discussion and complete description about the behaviors of the SAXS profiles very near T_{ODT} will be presented elsewhere.[12] It should be noted in Figure 4 that the ODT takes place in the same temperature interval both in the cooling and heating cycle: there is almost no hysterysis in this system with the time scale of observation employed here, implying that two-phase coexistence is an equilibrium phenomenon.

The temperature-variation of the SAXS profiles for SS-7 shows the similar trends to that for OSI-3 as shown in Figure 4, though it is not presented here. The T_{ODT} of SS-7 was determined as 141−145 °C.

III-2. Time-Resolved SAXS Observation for the Ordering Process. Figure 6 shows the time-evolution of the SAXS profiles after quenching OSI-3 from T_i = 172 °C to T_f = 97.0 °C just below T_{ODT} in the ordered state. The solid lines through the data points are just drawn for visual guides. Here we define the quench depth, ΔT, as

$$\Delta T \equiv T_{ODT,H} - T_f \qquad (4)$$

where $T_{ODT,H}$ is the onset temperature of the ordering from the disordered state, at which the σ_q^2 obtained from the static SAXS experiment in the cooling cycle decreases drastically. Figure 4 shows that the $T_{ODT,H}$ of OSI-3 is 100.1 °C; hence, ΔT in the case of the T-drop to 97.0 °C is 3.1 °C.

After the rapid quench of the specimen, the SAXS intensity increases with time t as follows. The SAXS profile first changes from that at the initial temperature 172 °C (dashed line) to that at 100.1 °C (dotted line) within 30 s which is the shortest time covered in this experiment, though the profile at 30 s is not shown here. After the profile reaches that at 100.1 °C, almost no change occurs in the SAXS profile as shown in the profiles at 90 and 360 s. After this period, the SAXS profile starts to change with time t. Here it should be mentioned that there are two characteristic wavenumbers q_{cS} and q_{cL} in Figure 6: the intensity increases at $q_{cS} < q < q_{cL}$, while it decreases outside the q range.

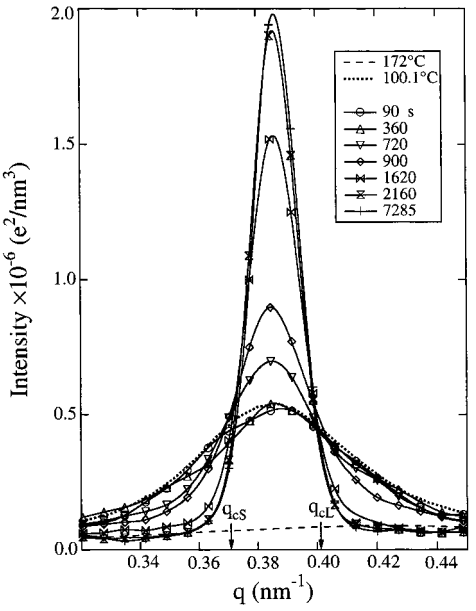

Figure 6. Time evolution of the SAXS profiles after quenching OSI-3 to 97.0 °C. The solid lines through the data points are for visual guides. The profiles drawn by the dash and dotted lines show those of OSI-3 at 172 °C, which is the initial temperature, and at 100.1 °C, which is the temperature very close to the T_{ODT} in the disordered state, respectively.

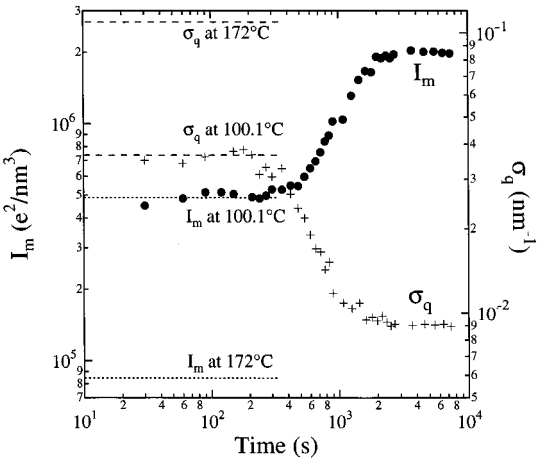

Figure 7. Time evolution of the values I_m and σ_q, after quenching OSI-3 from 172 °C far above the T_{ODT} to 97.0 °C just below the T_{ODT}. The horizontal dotted lines show the values I_m at 172 and 100.1 °C, and the dashed lines show the values σ_q at 172 and 100.1 °C for OSI-3.

Figure 7 gives the time-evolution of I_m and σ_q after quenching OSI-3 from T_i = 172 °C to T_f = 97.0 °C. The horizontal dotted lines show the equilibrium values of I_m at 172 and 100.1 °C, and the dashed lines show those of σ_q at 172 and 100.1 °C. This figure shows that the values I_m and σ_q at 30 s are almost equal to the equilibrium values at 100.1 °C which is the temperature just above the T_{ODT} (see Figure 4), indicating that the values I_m and σ_q change from the equilibrium values at 172 °C to those at 100.1 °C within 30 s after T-drop, though this change could not be observed in our experiments. The value I_m increased by six times within 30 s after T-drop. After the values I_m and σ_q reach the equilibrium values at 100.1 °C, they remain unchanged as long as ca. 400 s. After 400 s, the values I_m and σ_q

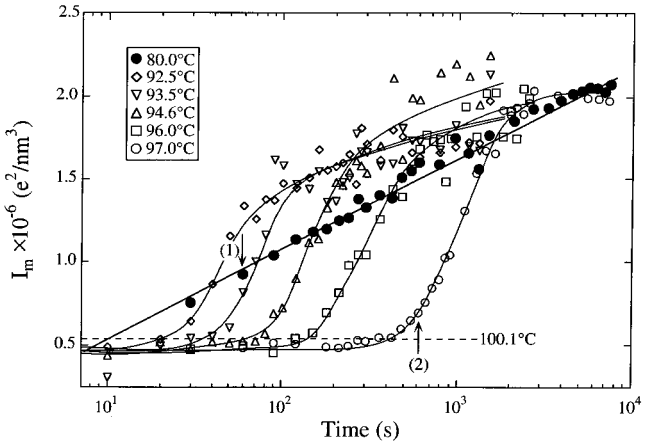

Figure 8. Time evolution of the value I_m after quenching OSI-3 from 172 °C above the T_{MF} to 97.0, 96.0, 94.6, 93.5, 92.5, and 80.0 °C below the T_{ODT}. The horizontal dashed line shows the value I_m at 100.1 °C for OSI-3. The solid lines through the data points are drawn for visual guides.

then start to increase and reach constant values at ca. 3000 s.

Figure 8 gives the time-evolution of the value I_m after quenching OSI-3 from T_i = 172 °C to T_f = 97.0, 96.0, 94.6, 93.5, 92.5, and 80.0 °C. The quench depth, ΔT, defined by eq 4 for each T_f is 3.1, 4.1, 5.7, 6.6, 7.6, and 20.1 °C, respectively. The horizontal dashed line shows the equilibrium value of I_m at 100.1 °C. Each solid line through the data points is drawn for a visual guide. It is worth noting in Figure 8 that the every time-evolution curve of the I_m in the time region where the I_m values start to increase shows almost same trend, except for 80.0 °C, though there are disparities in the late stage where the I_m at each T_f approach constant value in a different manner. Moreover it appears that, after T-drop, the I_m at each T_f rapidly increases from the initial value at T_i to the value equilibrium at 100.1 °C, and remains at that value at 100.1 °C for a certain period, except for the I_m at 80.0 °C. Here it should be mentioned that it takes ca. 50 s for the specimen to reach the set temperature as shown in Figure 3. Hence the ordering at 92.5 and 93.5 °C, which proceeds very fast, cannot not be regarded as the isothermal ordering.

In Figure 8, the time evolution of the value I_m at 80.0 °C, which changes gradually with increasing time, is quite different from that at the other temperatures. To compare the ordering of OSI-3 at 80.0 °C to that at 97.0 °C, the time-change in the SAXS profiles after the T-drop to 80.0 °C is given in Figure 9. In Figure 9, it is found that the scattered intensity increases only in the q range close to q_m, while it decreases outside this q range, the trend of which is approximately the same as that in Figure 6.

Figure 10 gives the time evolution of the I_m after quenching the different SI diblock copolymer, SS-7, which is also a nearly symmetric block copolymer (see Table 1), from 187 °C to 140 and 121 °C. The ordering of SS-7 is so fast that an incubation period could not be clearly observed before I_m starts to increase, but the trend of the time changes in I_m is similar to that at 97.0 °C for OSI-3 rather than that at 80.0 °C.

III-3. TEM Observations for the Ordering Process. The TEM micrograph taken at 90 s after quenching OSI-3 to 80.0 °C is given in Figure 11a. The state when the observation was done is shown by arrow 1 in Figure 8. To highlight the ordered grains composed of

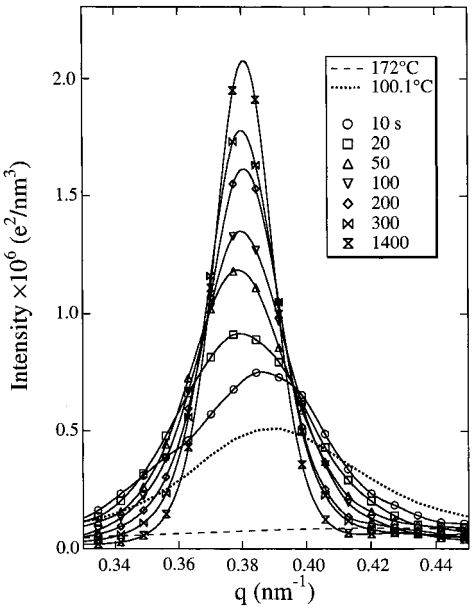

Figure 9. Time evolution of the SAXS profiles after quenching OSI-3 to 80.0 °C. The solid lines through the data points are drawn for visual guides. The profiles drawn by the dash and dotted lines show the profiles of OSI-3 at 172 °C, which is the initial temperature, and at 100.1 °C, which is the temperature very close to the T_{ODT} in the disordered state, respectively.

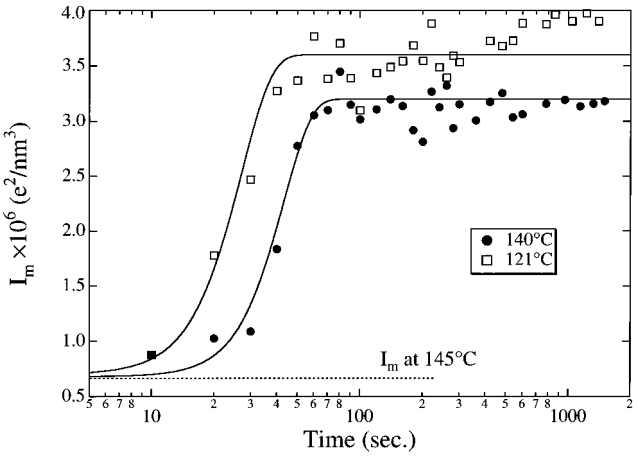

Figure 10. Time evolution of the value I_m after quenching SS-7 from 187 °C above the T_{ODT} to 140 and 121 °C below the T_{ODT}. The horizontal dotted line shows the value I_m at 145 °C for SS-7 which is the temperature very close to the T_{ODT} in the disordered state. The solid lines through the data points are drawn for visual guides.

the lamellar microdomain, the outlines of a few large grains are traced by white lines in the lower panel (b), although there are many grains which are left without markings. In Figure 11 it is interesting to note that the lamellar grains with a more or less sharp interface exist in the matrix of the less ordered phase; i.e., the lamellar grains and the less ordered phase coexist in Figure 11. To compare this micrograph with that obtained during the ordering at 97.0 °C, the TEM micrograph taken at 630 s after quenching OSI-3 to 97.0 °C is shown in Figure 12. The state when the observation was done is shown by arrow 2 in Figure 8. In Figure 12, it is also found that the lamellar grain with a sharp interface exists in the matrix of the less ordered phase, indicating that the ordered phase (grains) having a lamellar structure with a long-range order and the less ordered phase coexist at 630 s after quenching to

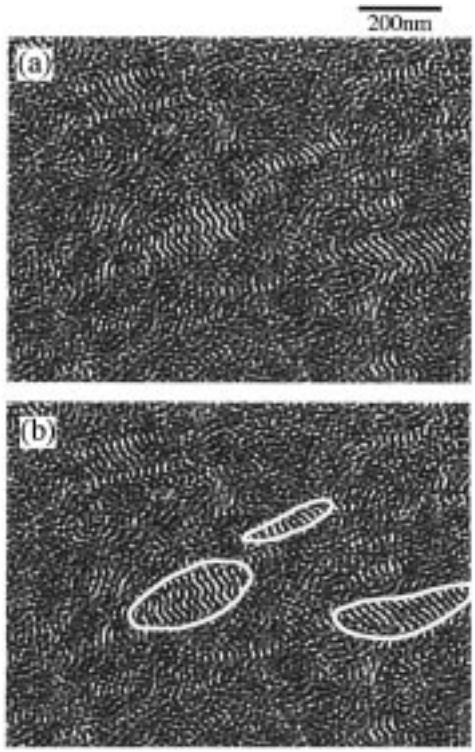

Figure 11. Transmission electron micrograph taken at 90 s after *T*-drop to 80 °C for OSI-3. The upper and lower panels show just the same image. To highlight the ordered grains composed of the lamellar microdomains, the outlines of a few grains are traced by white lines in the lower panel.

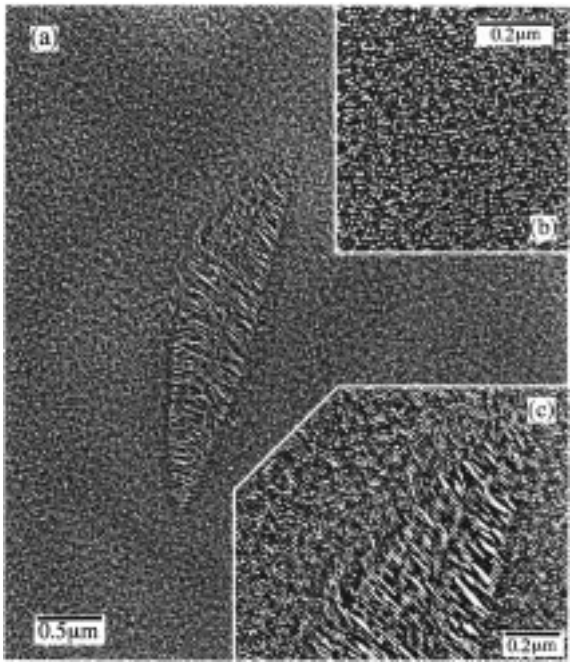

Figure 12. Transmission electron micrograph taken at 630 s after *T*-drop to 97.0 °C for OSI-3. Insets b and c high-light the disordered and ordered phases in picture a, respectively.

97.0 °C. Furthermore, Figures 11 and 12 show that the shape of the lamellar grains is very anisotropic: the size along the lamellar normals is much larger than that parallel to the lamellar interfaces. This feature is consistent with the prediction by Hohenberg and Swift.[4] The precise discussion about the shape of the grains will be presented elsewhere.[29]

It is noted that the anisotropic grains during the ordering process were found by using depolarized light scattering by Dai et al.[23] However the microdomain structure in their study is hexagonally packed cylinders but not lamellar. The shapes of the ordered grains in the matrix of the disordered phase highly depend on the type of the microdomains, because the anisotropy of the interfacial free energy between the grain and matrix, which is the origin for the anisotropy of the grain shape, depends on the symmetry of the microdomain structures.

IV. Discussion

IV-1. Ordering Mechanism at the Temperature Close to T_{ODT}. Figures 6 and 7 show that after *T*-drop to 97.0 °C the SAXS profile of OSI-3 first changes rapidly from that at the initial temperature 172 °C to that at 100.1 °C which is very close to the T_{ODT} in the disordered state. Although we could not observe this change in the SAXS profile with time, the SAXS profile before *T*-drop should take the one equilibrium at 172 °C and the SAXS profile at 30 s after *T*-drop to 97.0 °C is almost same as the one equilibrium at 100.1 °C, indicating that the SAXS profile had changed from that at 172 °C to that at 100.1 °C within 30 s. This change corresponds to the relaxation of the thermal concentration fluctuations from those at T_i in the mean-field disordered state to those at 100.1 °C which is very close to the T_{ODT} in the disordered state. Thus it is found that the relaxation of the thermal concentration fluctuations in the disordered state from those at 172 °C to those at 100.1 °C completed within 30 s. This result implies that the ordering process is independent of the initial temperature, because the system changes from the initial state to the state at the temperature just above the T_{ODT} before the formation of the ordered grains.

After the profile reaching the one equilibrium at 100.1 °C, almost no change occurs in the time interval of $30 < t < 400$ s. Here it should be noted that the temperature in the specimen reaches 97.0 °C within 50 s as shown in Figure 3. Hence the temperature was already equilibrated to 97.0 °C in this time region. Thus the system remains in the disordered state at 100.1 °C until about 400 s after *T*-drop, revealing the existence of the incubation period for the ordering process, and that the thermal concentration fluctuations in the incubation period are almost same as that at 100.1 °C. It should be mentioned that the scattered intensity from the supercooled disordered melt at 97.0 °C may be very close to that from the disordered melt at 100.1 °C. Thus the scattered intensity in the incubation period may be actually that from the supercooled disordered state at 97.0 °C.

After the incubation period, the SAXS profile starts to increase and reaches a constant, indicating that the formation of the lamellae starts and the system is approaching the steady state. At 7285 s after *T*-drop to 97.0 °C, the lamellae filled the whole sample space, as will be presented elsewhere.[29] Moreover in this stage, the intensity increases at $q_{cS} < q < q_{cL}$ but decreases at $q > q_{cL}$ or $q < q_{cS}$. This mode selection mechanism cannot be explained on the basis of the linearized theory of spinodal decomposition in the context of mean-field approximation and the *q* dependence of the Onsager transport coefficient.[30] This feature, together with the existence of the incubation

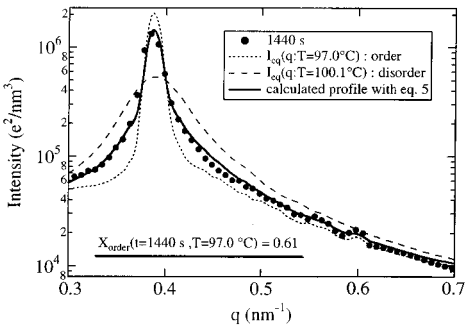

Figure 13. SAXS profile at 1440 s after quenching OSI-3 to 97.0 °C (filled circle). The profile drawn by the solid line shows the calculated profile by eq 5 with $X_{order}(t = 1440$ s; $T_f = 97.0$ °C) = 0.61. The profiles drawn by dotted and broken lines show the SAXS profiles of OSI-3 at 97.0 and 100.1 °C obtained from the static SAXS experiment in the heating cycle, respectively.

period, suggests that this ordering process is nucleation and growth process which is very much influenced by the random thermal force.[3−17] This conclusion is supported by the TEM picture in Figure 12. In Figure 12, the ordered and less ordered phases clearly coexist. Moreover the less ordered phase is apparently similar to the disordered phase very close to the ODT as will be shown in detail elsewhere,[17,29] indicating that the ordered and disordered phases coexist in Figure 12. It suggests that this ordering proceeds via nucleation and growth process rather than spinodal decomposition. The ordering proceeds via a growth of ordered grains at the expense of the disordered phase.

Thus it is found that the ordering of OSI-3 at 97.0 °C proceeds via a nucleation and growth process and consists of the following **three stages**: (I) The scattered intensity $I(q)$ changes rapidly from that at 172 to 100.1 °C within 30 s. The change in stage I corresponds to the relaxation of the thermal concentration fluctuations in the disordered state. (II) The profile $I(q)$ stays equal to that of the equilibrium value at 100.1 °C between 30 and 400 s. Stage II corresponds to the incubation period for the ordering process. (III) The profile $I(q)$ changes after 400 s and reaches a constant value at ca. 3000 s. The change in stage III corresponds to the growth of the lamellar grains at the expense of the disordered phase.

Furthermore we found that the SAXS profiles during the ordering of OSI-3 at 97.0 °C can be approximately expressed by:

$$I(q, t; T_f) = [1 - X_{order}(t; T_f)]I_{eq}(q; 100.1\ °C) + X_{order}(t; T_f)I_{eq}(q; T_f) \quad (5)$$

with $T_f = 97.0$ °C, just like an equilibrium scattering profile in the order−disorder coexistence region (see Figure 5), where $I(q, t; T_f)$ is the SAXS profiles during the ordering of OSI-3 at T_f, and $I_{eq}(q; 100.1$ °C) and $I_{eq}(q; T_f)$ were estimated from the SAXS profile of OSI-3 at 100.1 °C and T_f obtained from the static SAXS experiment in the heating cycle, respectively. The $X_{order}(t; T_f)$ is the volume fraction of the ordered lamellar phase at a given t after quenching OSI-3 to T_f.

Figure 13 demonstrates a typical example of the above analysis based on eq 5 where the SAXS profile of OSI-3 at 1440 s after T-drop to 97.0 °C (filled circles) is best-fitted by eq 5 with $X_{order}(t = 1440$ s; $T_f = 97.0$ °C) = 0.61 (solid line). The evidence that the SAXS profile is expressed by eq 5 means that the system during the ordering of OSI-3 is composed of the two phases: the ordered lamellar grains at 97.0 °C and the disordered phase at 100.1 °C. Thus we can separate the net scattering intensity into those from the two phases and estimate the volume fraction of the ordered phase X_{order} as a function of time during the ordering.

IV-2. Quench-Depth Dependence of the Ordering Process. (A) Shallow Quenches. In Figure 8, we observe that each curve for the time evolution of the value I_m shows an incubation period before an increase of the value I_m, and each curve has almost same behavior during the early stage of the ordering, except for the curve obtained at 80.0 °C: the ordering at each T_f proceeds via the three stages described in section IV-1. However it takes ca. 50 s for the specimen to reach the equilibrium temperature as shown in Figure 3, and the ordering process at 92.5 and 93.5 °C is not slow enough relative to the rate required to reach the equilibrium temperature so that the ordering at these temperatures cannot not be regarded as the isothermal ordering.

Despite the difficulty, we have tried to qualitatively compare the ordering processes of OSI-3 at 97.0, 96.0, 94.6, 93.5, and 92.5 °C. The time changes in I_m after T-drop to the respective temperatures are plotted as a function of the reduced time, $t/t_{1/2}$, in Figure 14, where $t_{1/2}$ is the time at which the value of I_m reaches $I_{m1/2}$ defined by $I_{m1/2} = (I_{m,100.1°C} + I_{m,Tf})/2$, where $I_{m,100.1°C}$ and $I_{m,Tf}$ are the equilibrium values of I_m at 100.1 °C and T_f obtained by the static SAXS experiment, respectively. It is found in Figure 14 that all the curves fall onto a master curve, except for the late stage. This fact suggests that the mechanism of the ordering at $92.5 < T_f < 97.0$ °C is essentially identical, though the ordering at 92.5 and 93.5 °C cannot be rigorously regarded as the isothermal ordering. The inset shows $t_{1/2}$ plotted as a function of ϵ^{-1}, where the quantity ϵ is the thermodynamic driving force for the ordering, defined as

$$\epsilon \equiv \frac{\chi_f - \chi_{ODT}}{\chi_{ODT}} \quad (6)$$

with χ_f and χ_{ODT} being the χ values at the temperatures T_f and T_{ODT}, respectively. The χ values are calculated by using the following equation obtained for OSI-3:[8]

$$\chi = -0.0237 + 34.1/T \quad (7)$$

The result reveals that $\log t_{1/2}$ linearly increases with ϵ^{-1}. This trend is consistent with the results obtained by Floudas[21] for the nearly symmetric SI diblock copolymer.

(B) Deep Quenches. In Figure 8, the ordering at 80.0 °C seems to be quite different from the others. Floudas et al.[20] reported that the ordering for the shallow quenches proceeds via nucleation and growth, but that for the deep quenches proceeds via spinodal decomposition. To clarify the ordering mechanism at 80.0 °C, we compare the time-evolution of the SAXS profiles after T-drop to 80.0 °C with that to 97.0 °C. In Figure 6, the SAXS profiles of OSI-3 after T-drop to 97.0 °C remain equal to the equilibrium profile in the disordered state at 100.1 °C for the incubation period, and after this period the intensity increases at $q_{cS} < q < q_{cL}$ and decreases outside this q range. The position of the q_m hardly shifted during the ordering. On the other hand, the SAXS profiles of OSI-3 after T-drop to

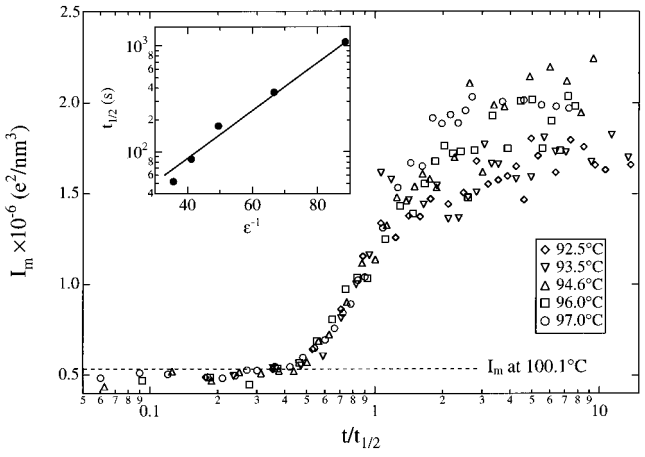

Figure 14. I_m at 97.0, 96.0, 94.6, 93.5, and 92.5 °C, plotted as a function of $t/t_{1/2}$ for OSI-3 The inset shows the $t_{1/2}$ plotted as a function of $\epsilon^{-1}=\{(\chi_f - \chi_{ODT})/\chi_{ODT}\}^{-1}$. χ_f is the χ value at T_f.

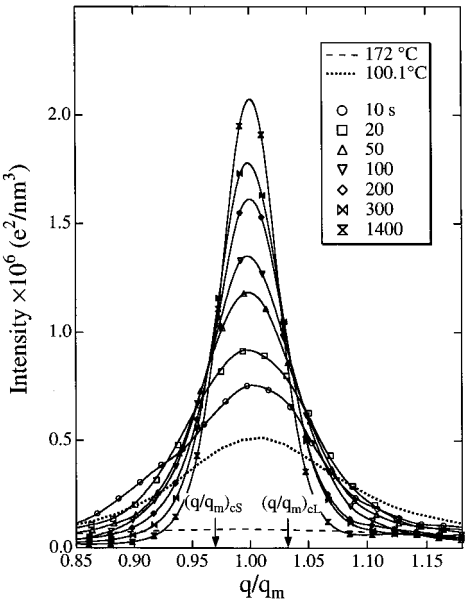

Figure 15. Time evolution of the SAXS profiles after quenching OSI-3 to 80.0 °C plotted as a function of q/q_m. The solid lines through the data points are drawn for visual guides. The profiles drawn by the dash and dotted lines show those of OSI-3 at 172 °C, which is the initial temperature, and at 100.1 °C, which is the temperature very close to the T_{ODT} in the disordered state, respectively.

80.0 °C start to change without an incubation period as shown in Figures 8 and 9. Nevertheless the scattered intensity increases only in the q range close to q_m, and it decreases outside this q range (Figure 9), the trend of which is approximately the same as that found in Figure 6. After scaling q with the time-dependent q_m, this trend becomes more evident, as shown in Figure 15. In this figure, there are two characteristic scaled wavenumbers, $(q/q_m)_{cS}$ and $(q/q_m)_{cL}$: the intensity increases at $(q/q_m)_{cS} < q/q_m < (q/q_m)_{cL}$ and decreases outside this region. The decrease of q_m with time is a phenomenon relevant to ordering at deep quenches and is a consequence of stretching of chains in ordered lamellae. As mentioned in section IV-1, this mode selection mechanism cannot be explained on the basis of the mean-field linearized theory of spinodal decomposition. Moreover the lamellar grains exist in the matrix of the less ordered phase; i.e., the lamellar grains and the less ordered phase coexist during the ordering at 80.0 °C as shown in Figure 11. Thus the ordering of OSI-3 at 80.0 °C, as well as that at the other temperatures, is anticipated to proceed via nucleation and growth over the time scale covered in this study, contrary to the report by Floudas et al.[20]

At this moment, we cannot answer why the time evolution of I_m at 80.0 °C is quite different from that at the other temperatures.[31] However, there is a possibility that the difference in the time-evolution of I_m at 80.0 °C and the other temperatures results from the vitrification of the PS-rich phase in the ordering process. Figure 10 shows the time-evolution of I_m for SS-7 after T-drop to 140 and 121 °C. The T_{ODT} of SS-7 is higher than that of OSI-3 (see Table 1). The ϵ values expressed by eq 6 for the ordering of SS-7 at 140 and 121 °C are 0.0170 and 0.0859, respectively, which are very close to those for the ordering of OSI-3 at 97.0 and 80.0 °C (0.0113 and 0.0768, respectively). Thus the ordering of OSI-3 at 97.0 and 80.0 °C should be thermodynamically almost identical with that of SS-7 at 140 and 121 °C, respectively. In Figure 10 it is easily found that the time evolution of I_m for SS-7 at 121 and 140 °C, are similar to that for OSI-3 at 97.0 °C: the I_m values of SS-7 at 121 °C do not show the linear relationship with log t, as shown in the ordering of OSI-3 at 80.0 °C. This evidence may indicate that the ordering of OSI-3 at 80.0 °C is strongly affected by mobility and hence seemingly by the vitrification. Here it should be mentioned that the T_g of OSI-3 estimated by the DSC measurement is 61 °C as shown in section II, which is lower than 80 °C. However T_g highly depends on the state of the system,[24] and the vitrification may come into play even in the ordering process at 80.0 °C.

The SAXS profiles in the course of the ordering at 80.0 °C cannot be expressed in terms of a weighted average of the static profiles at 100.1 and 80.0 °C, contrary to the fact that the SAXS profiles during the ordering at 97.0 °C can be expressed by eq 5. It means that the system is not composed of the lamellar grains that develop at $t \rightarrow \infty$ at 80.0 °C and the disordered phase at 100.1 °C. Moreover the less ordered phase in Figure 11 appears to be slightly different from the disordered phase at the temperature very close to T_{ODT}: it is more likely to be the "distorted ordered" phase which is the ordered phase but not grown into lamellar grains with a substantial long-range order, though it is difficult to unequivocally identify whether the less ordered phase in Figure 11 corresponds to the disordered phase or the distorted ordered phase. Thus it might be conceivable that the ordering mechanism at 80.0 °C is different from that at the other temperatures: at temperatures between 97.0 and 92.5 °C the lamellar grains appear in the disordered phase and develop with time by a nucleation and growth process, while at 80.0 °C the ordering takes place via a two-step mechanism; the first-step ordering very rapidly forms the "distorted ordered" phase from the disordered phase, and the second-step ordering slowly develops grains of lamellae with a long-range order. The second ordering may correspond to the slow time-evolution of I_m for OSI-3 at 80.0 °C.

Koppi et al.[32] and Tepe et al.[33] estimated that the stability limit temperature, below which the spontaneous ordering or the exceedingly rapid nucleation takes place, exists 11 and 16 °C lower than T_{ODT} for the poly(ethylene−propylene) (PEP)-*block*-poly(ethylethylene)

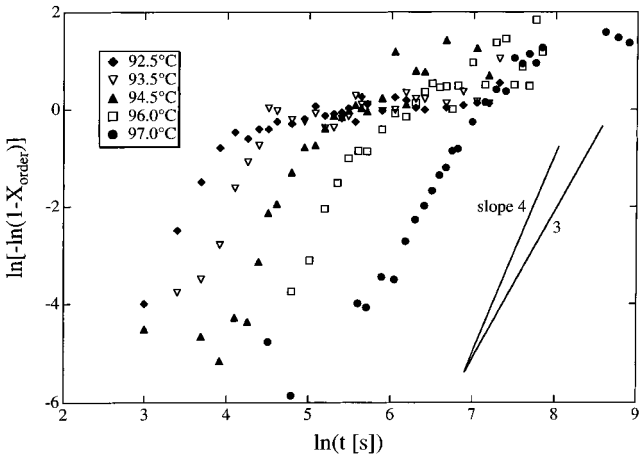

Figure 16. Avrami plots of the quantity X_{order} for OSI-3, obtained by fitting eq 5 with the time-resolved SAXS profiles.

(PEE) diblock and the PEP-*block*-PEE-*block*-PEP triblock copolymer, respectively. This temperature (16 °C) is smaller than the quench depth, ΔT (20.1 °C), for the ordering at 80.0 °C. The ordering in the first-step from the disordered phase to the "distorted ordered" phase may proceed via the spontaneous ordering or the exceedingly rapid nucleation, as predicted by them.

Thus we cannot make a definite conclusion in this case. More analyses will be needed in future work. However, we must remember that the lamellar grains and the less ordered phase coexist during the ordering at 80.0 °C as shown in Figure 11. Thus we can clearly state that the lamellar grains are developed from the disordered state or the "distorted ordered" state by nucleation and growth process: the lamellar microdomains *do not* appear directly from the disordered state by the spinodal decomposition.

IV-3. Avrami Analysis. As described in section IV-1, the SAXS profiles during the ordering of OSI-3 at 97.0 °C were able to be expressed in terms of a weighted average of the equilibrium profile at 100.1 and 97.0 °C. The other profiles during ordering at 96.0, 94.6, 93.5, and 92.5 °C can be also well-expressed by eq 5. The quantity $X_{order}(t; T_f)$ thus obtained were analyzed by the Avrami equation[34]

$$X_{order} = 1 - \exp(-zt^n) \tag{8}$$

where z is constant and n is the Avrami exponent. The Avrami exponent is related to the dimensionality and the type of the nucleation (homogeneous or heterogeneous).

Figure 16 gives the Avrami plot ($\ln[-\ln(1 - X_{order})]$ vs $\ln(t)$ plot) for the ordering of OSI-3 at 97.0, 96.0, 94.6, 93.5, and, 92.5 °C. If the ordering process obeys eq 8, $\ln[-\ln(1 - X_{order})]$ shows a linear relationship with $\ln(t)$, and the Avrami exponent can be obtained from the slope. In Figure 16 it is easily found that in every case, $\ln[-\ln(1 - X_{order})]$ change linearly with $\ln(t)$ except for the late stage. Moreover the slope of the each curve is almost same, revealing that the mechanism of the ordering process of OSI-3 at $92.5 \leq T_f \leq 97.0$ °C is essentially identical, though the time scale of the ordering is quite different. Thus the Avrami exponent, n, for the ordering process of OSI-3 at $92.5 \leq T_f \leq 97.0$ °C is determined as the value between 3 and 4, though we could not determine the precise value of n because of the limited data points. This value of n is consistent with the result obtained by Floudas et al.[21] in the T-drop experiments for the nearly symmetric SI diblock copolymer at shallow quenches.

If $n = 4$ is adopted as the Avrami exponent, one might conclude that the ordering proceeds via the three-dimensional growth with homogeneous nucleation, and if $n = 3$, one might conclude that it proceeds via the two-dimensional growth with homogeneous nucleation or the three-dimensional growth with heterogeneous nucleation. Here it should be mentioned that, in the heterogeneous nucleation process, the nucleation is induced by impurities in the system, and the number density of the nuclei should be constant for all the T-drop measurements, if the number density of the impurities is independent of temperature. On the contrary, the number density of the lamellar grains at 97.0 °C in Figure 12 is quite different from that at the other temperatures, as shown in Figure 11 and as will be presented elsewhere.[29] At a given T_f, the number density of the grains should be independent of time if the nucleation process is heterogeneous. On the contrary, our TEM observation indicates that it tends to increase with time. Thus the nucleation process encountered in OSI-3 is expected to be homogeneous nucleation.

Moreover it should be noted that the interpretation of the Avrami exponent in the previous work[21] was based on the assumption that the ordered grains grow isotropically. However, the shape of the lamellar grains in the matrix of the disordered phase are very anisotropic as shown in Figures 11 or 12, and the growth rate is expected to be anisotropic; i.e., the growth rate parallel to the lamellar normal should be different from that perpendicular to it. If the anisotropy is not too large, the relationship between the Avrami exponent and the type of the nucleation or the dimensionality of the grain growth mentioned above can be appropriate.[35] However when the ordered grains are highly anisotropic, such as is the case in the present study, the Avrami exponent changes with time and the value of Avrami exponent is smaller than that for isotropic growth:[36,37] the Avrami exponent for homogeneous nucleation in three-dimensional space with anisotropic growth rate becomes smaller than 4. Thus the TEM pictures and the Avrami exponent of between 3 and 4 in the present study at $97.0 \leq T_f \leq 92.5$ °C reveal that the ordering of a nearly symmetric diblock copolymer proceeds via *anisotropic* three-dimensional growth with *homogeneous* nucleation.

Here it should be noted that Floudas et al.[21] and Rosedale et al.[19] conclude that the ordering of the symmetric diblock copolymers proceeds via *heterogeneous* nucleation and *isotropic* three-dimensional growth by using the Avrami analysis and Fredrickson and Binder theory.[13] However Fredrickson and Binder theory also assumes that the interfacial tension of the grains of lamellae in the matrix of the disordered phase is directionally independent and hence the grains are spherically symmetric. On the contrary, the actual shape of the lamellar grains in the matrix of the disordered phase is highly anisotropic,[16,17,29] and the growth rates parallel and perpendicular to the lamellar normal should be different. Thus the prediction of Fredrickson and Binder theory involves some problems. From experimental viewpoints we need further quantitative information on the aspect ratio of the lamellar grain parallel and perpendicular to the lamellar normal

and the ratio of the growth rates in the two principal directions. These features should be studied in future works.

V. Concluding Remarks

We have investigated the ordering dynamics of a nearly symmetric diblock copolymer of a polystyrene-*block*-polyisoprene, having a lamellar microdomain structure in the ordered state, by quenching the specimens from the mean-field disordered state to the ordered state at various quench depths. The ordering process was observed by the time-resolved SAXS and TEM. It is found that the ordering of a nearly symmetric block copolymer at shallow quenches proceeds via nucleation and growth process with the three stages. The scattering behaviors and the states of the system in the each stage of the ordering are as follows: (I) the scattered intensity increases rapidly from the initial one to the one at equilibrium at 100.1 °C in the disordered state very close to T_{ODT}, within the shortest time covered in this experiment, during which the thermal concentration fluctuations relax rapidly from the initial state to the equilibrium disordered state at the temperature very close to T_{ODT}; (II) the scattered intensity does not change for a certain incubation period, during which the system stays in the disordered state at the temperature very close to T_{ODT}; (III) the scattered intensity increases at $q_{cS} < q < q_{cL}$ but decreases at $q > q_{cL}$ or $q < q_{cS}$, during which the formation of the lamellar microdomains starts and the system eventually approaches a steady state. Moreover the SAXS profiles in stage III can be approximately expressed in terms of a weighted average of the equilibrium profile at 100.1 °C and that steady at T_f, indicating that the system during the ordering of OSI-3 is composed of the two phases: the ordered lamellar grains at T_f and the disordered phase at 100.1 °C.

On the other hand, the time evolution of the value I_m after quenching OSI-3 to 80.0 °C (corresponding to a relatively deep quench) showed a trend different from that found at the shallow quenches. However the scattered intensity after *T*-drop to 80.0 °C increases in the q range close to q_m, but decreases outside the q range, the trend of which is essentially same as that in stage III at the shallow quenches. These evidences and the TEM image in Figure 11 imply that the ordering of the lamellar microdomains at 80.0 °C also proceeds via a nucleation and growth process.

The Avrami analysis on the time-change in the volume fraction of the ordered phase after quenching OSI-3 to the temperatures between 92.5 and 97.0 °C showed that the Avrami exponent gives the almost same value, $3 < n < 4$, meaning that the ordering mechanism at these quenches is essentially same. This value of the Avrami exponent together with the TEM pictures during the ordering suggest that the ordering proceeds via the *anisotropic* three-dimensional growth with *homogeneous* nucleation.

Acknowledgment. This work was supported in part by Research Fellowships of the Japan Society for the Promotion of Science (JSPS) for Young Scientists (6608) and by a Grant-in-Aid for JSPS fellows (00086608) and Scientific Research on Priority Area, "Cooperative Phenomenon in Complex Liquids" (07236103) from the Ministry of Education, Science, Sports, and Culture, Japan.

References and Notes

(1) See, for example, a review article: Hashimoto T. *Thermoplastic Elastomers*; Legge, N. R., Holden, G. R., Schroeder, H. E., Eds.; Hanser: Vienna: 1987, 1st ed., Chapter 12, Section 3; 1996, 2nd ed., Chapter 15A and references therein.
(2) Leibler, L. *Macromolecules* **1980**, *13*, 1602.
(3) Fredrickson, G. H.; Helfand, E. *J. Chem. Phys.* **1987**, *87*, 697.
(4) Hohenberg, P. C.; Swift, J. B. *Phys. Rev. E.* **1995**, *52*, 1828.
(5) Bates, F. S.; Rosedale, J. H.; Fredrickson, G. H. *J. Chem. Phys.* **1990**, *92*, 6255.
(6) Wolff, T.; Burger, C.; Ruland, W. *Macromolecules* **1993**, *26*, 1707.
(7) Rosedale, J. H.; Bates, F. S.; Almdal, K.; Mortensen, K.; Wignall, D. *Macromolecules* **1995**, *28*, 1429.
(8) Sakamoto, N.; Hashimoto, T. *Macromolecules* **1995**, *28*, 6825.
(9) Floudas, G.; Pispas, S.; Hadjichristidis, N.; Pakula, T.; Erukhimovich, I. *Macromolecules* **1996**, *29*, 4142.
(10) Brazovskii, A. *Sov. Phys. JETP* **1975**, *41*, 85.
(11) Hashimoto, T.; Ogawa, T.; Sakamoto, N.; Ichimiya, M.; Kim, J. K.; Han, C. D. *Polymer* **1998**, *39*, 1573.
(12) Koga, T.; Koga, T.; Hashimoto, T. Manuscript in preparation.
(13) Fredrickson, G. H.; Binder, K. *J. Chem. Phys.* **1989**, *91*, 7265.
(14) Schuler, M.; Stühn, B. *Macromolecules* **1993**, *26*, 112.
(15) Stühn, B.; Vilesov, A.; Zachmann, H. G. *Macromolecules* **1994**, *27*, 3560.
(16) Hashimoto, T.; Sakamoto, N. *Macromolecules* **1995**, *28*, 4779.
(17) Hashimoto, T.; Sakamoto, N.; Koga, T. *Phys. Rev. E* **1996**, *54*, 5832.
(18) Hajduk, D. A.; Tepe, T.; Takenouchi, H.; Tirrell, M.; Bates, F. S. *J. Chem. Phys.* **1998**, *108*, 326.
(19) Rosedale, J. H.; Bates, F. S. *Macromolecules* **1990**, *23*, 2329.
(20) Floudas, G.; Hadjichristidis, N.; Iatrou, H.; Pakula, T.; Fischer, E. W. *Macromolecules* **1994**, *27*, 7735.
(21) Floudas, G.; Pakula, T.; Fischer, E. W.; Hadiichristidis, N.; Pispas, S. *Acta Polym.* **1994**, *45*, 176.
(22) Floudas, G.; Fytas, G.; Hadichristidis, N.; Pitsikalis, M. *Macromolecules* **1995**, *28*, 2359.
(23) Dai, H. J.; Balsara, B. A.; Garetz, B. A.; Newstein, M. C. *Phys. Rev. Lett.* **1996**, *77*, 3677.
(24) It is very difficult to determine the T_g of the polystyrene- (PS-) rich phase in the ordered state for the block copolymer studied. This is because it takes extremely long time for the block copolymer to reach the equilibrium ordered state as shown in the time-evolution of the I_m at 80 °C for OSI-3 (see Figure 8 in this manuscript). The T_g of the PS-rich phase in the well-ordered microdomains may be different from that in the disordered phase or distorted ordered phase; i.e., the T_g should depend on the state of order, e.g., the volume fraction of the disordered phase or distorted ordered phase coexisting with the well-ordered lamellar phase. Thus the T_g measured by the DSC, etc., depends on the initial state of the sample and the condition of the measurement.
(25) Fujimura, M.; Hashimoto, T.; Kawai, H. *Mem. Fac. Eng., Kyoto Univ.* **1981**, *43* (2), 224.
(26) Hashimoto, T.; Suehiro, S.; Shibayama, M.; Saijo, K.; Kawai, H. *Polym. J.* **1981**, *13*, 501.
(27) Suehiro, S.; Saijo, K.; Ohta, Y.; Hashimoto, T.; Kawai, H. *Anal. Chim. Acta* **1986**, *189*, 41.
(28) Hendricks, R. W. *J. Appl. Crystallogr.* **1972**, *5*, 315.
(29) Sakamoto, N.; Hashimoto, T. *Macromolecules*, in press.
(30) Kawasaki, K.; Sekimoto, K. *Macromolecules* **1989**, *22*, 3063.
(31) The slow ordering at a deep quench was reported by Harkless et al.[38] In their paper, the time-change of the volume fraction of the ordered phase in the block copolymer can be described by the Avrami equation (eq 8),[34] with $n = 4$ in the early stage of the ordering at a shallow quench, while $n = 1$ in the late stage of the ordering at a shallow quench and in all the stage at a deep quench; i.e., the ordering in the latter is much slower than that in the former. The value of the Avrami exponent, $n = 1$, is interpreted to be due to the effects of the site saturation and impingement. The Avrami exponent $n = 1$ at a deep quench was also reported by Hajduk et al.[18] Unfortunately, the Avrami exponent of OSI-3 at 80.0 °C could not be determined, because the SAXS profiles at 80.0 °C cannot be expressed in terms of a weighted average of the equilibrium profiles at 100.1 and 80.0 °C. However it should be noted that the ordered lamellar grains seem not to fill all

the sample space in Figure 11. The considerable space for the nucleation site or grain growth, seems to remain in Figure 11. Thus the ordering of OSI-3 at 80.0 °C could not be explained by site saturation and impingement.

(32) Koppi, K. A.; Tirrell, M.; Bates, F. S. *Phys. Rev. Lett.* **1993**, *70*, 1449.

(33) Tepe, T.; Hadjuk, D. A.; Hillmyer, M. A.; Weimann, P. A.; Tirrell, M.; Bates, F. S. *J. Rheol.* **1997**, *41*, 1147.

(34) Avrami, M. J. *J. Chem. Phys.* **1939**, *7*, 1103.

(35) Weinberg, M. C.; Birnie, D. P., III *J. Non-Cryst. Solids* **1995**, *189*, 161.

(36) Shepilov, M. P.; Baik, D. S. *J. Non-Cryst. Solids* **1994**, *171*, 141.

(37) Weinberg, M. C.; Birnie, D. P., III *J. Non-Cryst. Solids* **1996**, *202*, 290.

(38) Harkless, C. R.; Singh, M. A.; Nagler, S. E.; Stephenson, G. B.; Jordan-Sweet, J. L. *Phys. Rev. Lett.* **1990**, *64*, 2285.

MA9717202